Check for updates

Chemistry
A European
Journal

Chemistry Europe
European Chemical Societies Publishing

Accepted Article

Title: A Remarkable Fluorescence Quenching Based Amplification in ATP Detection through Signal Transduction in Self-assembled Multivalent Aggregates

Authors: Rakesh Biswas, Sumit Naskar, Surya Ghosh, Mousumi Das, and Supratim Banerjee

This manuscript has been accepted after peer review and appears as an Accepted Article online prior to editing, proofing, and formal publication of the final Version of Record (VoR). This work is currently citable by using the Digital Object Identifier (DOI) given below. The VoR will be published online in Early View as soon as possible and may be different to this Accepted Article as a result of editing. Readers should obtain the VoR from the journal website shown below when it is published to ensure accuracy of information. The authors are responsible for the content of this Accepted Article.

To be cited as: *Chem. Eur. J.* 10.1002/chem.202002648

Link to VoR: https://doi.org/10.1002/chem.202002648

WILEY-VCH

10.1002/chem.202002648

WILEY-VCH

COMMUNICATION

A Remarkable Fluorescence Quenching Based Amplification in ATP Detection through Signal Transduction in Self-assembled Multivalent Aggregates

Rakesh Biswas, Sumit Naskar, Surya Ghosh, Mousumi Das,* and Supratim Banerjee*

R. Biswas, S. Naskar, S. Ghosh, Prof. Dr. M. Das and Prof. Dr. S. Banerjee
Department of Chemical Sciences
Indian Institute of Science Education and Research Kolkata
Mohanpur, West Bengal, India
E-mail: supratim.banerjee@iiserkol.ac.in, mousumi@iiserkol.ac.in

Supporting information for this article is given via a link at the end of the document

Abstract: Signal transduction is essential for the survival of living organisms as it allows them to respond to the changes in external environments. In artificial systems, signal transduction has been exploited for the highly sensitive detection of analytes. Herein, we report a remarkable signal transduction, upon ATP binding, in the multivalent fibrillar nanoaggregates of anthracene conjugated imidazolium receptors. The aggregates of one particular amphiphilic receptor sensed ATP in high pM concentrations with one ATP molecule essentially quenching the emission of thousands of receptors. A cooperative merging of the multivalent binding and signal transduction led to this superquenching and translated to an outstanding enhancement of more than a million-fold in the sensitivity of ATP detection by the nanoaggregates; in comparison to the "molecular" imidazolium receptors. Furthermore, an exceptional selectivity to ATP over other nucleotides was demonstrated.

Nature utilizes multivalency[1] to govern molecular recognition events[2] which are key to many essential biological functions including cellular adhesion and signal transduction.[3] In signal transduction, a selective and amplified chemical response is generated in the presence of a particular stimulus.[4] Inspired by the high efficiency of the natural signal transduction processes, artificial systems have been developed and exploited for analyte detection at ultralow concentrations. The signal amplification in artificial systems is typically accomplished either through enzyme catalyzed reactions or by employing multivalent binding in which a single binding event affects the properties of multiple receptors.[5] The chemo-sensing by conjugated polymer electrolytes (CPEs), macromolecules with π-conjugated backbone and ionic side groups, represents one of the prominent examples of signal transduction by multivalent binding.[6] The conjugated backbone in these "molecular wires" helps in amplifying the binding event through an efficient exciton migration.[7] We were interested in designing modular self-assembled systems which would integrate the features of multivalency and signal amplification for the detection of bio-analytes. The self-assembly route reduces the tedious and time-consuming protocols often required for the synthesis of CPEs to a great extent and also offers modularity in terms of the morphology. Because of these beneficial features, self-assembled multivalency,[8] in which nano-scale, high affinity multivalent arrays are created through the self-assembly of smaller components, has emerged as a key technique for the detection and binding of DNA,[9] heparin,[10] proteins,[11] carbohydrates[12] and other analytes.[13]

The bio-analyte of our choice was ATP, a molecule with prime importance in cell biology. It is the universal energy currency in cells and plays pivotal roles in many cellular processes including active transport and cell division.[14] The synthetic probes employed for ATP detection typically relies on electrostatic interactions and/or H-bonding.[15] A number of metal ion-based receptors,[15,16] metal-free pure organic receptors[15,17] and aptamers[18] have been developed for ATP detection. In addition to these "molecular" receptors, multivalent binding of ATP and other phosphates have been reported on the micellar and vesicular interfaces, monolayers, *etc*.[19]

Imidazolium-based luminescent cyclophanes, podands and tweezers are known for ATP binding[20] by utilizing a combination of electrostatic as well as (C-H)$^{+}$…O^{-} hydrogen bonds. These receptors were predominantly "molecular" in nature with multiple imidazolium groups connected at different positions of anthracene, pyrene, *etc*. The cavity/cleft created by the arrangement of the imidazolium groups in space led to the binding of the nucleotides through multiple electrostatic interactions. Additionally, the aromatic moieties in the receptors presented stacking interactions with the nucleobases to further stabilize the complexes. We present here a fundamentally different approach in which rather than covalently linking the imidazolium receptors, they are organized through supramolecular self-assembly. Towards this goal, we employ a series of imidazolium-based receptors (**AImN**, N = the number of carbons in the alkyl chain, Figure 1) for ATP binding. The self-assembly and photophysical properties of the **AImN** receptors in aqueous media were governed by the length of the hydrophobic *n*-alkyl segment. Supramolecular nano-fibrillar aggregates were formed with N≥10 chains (Figure 1), whereas the smaller chain derivatives (N≤6) remained in non-assembled states. The aggregates exhibited greenish excimeric emissions which underwent pronounced quenching in the presence of ATP. Although the quenching was noted for all the three amphiphilic

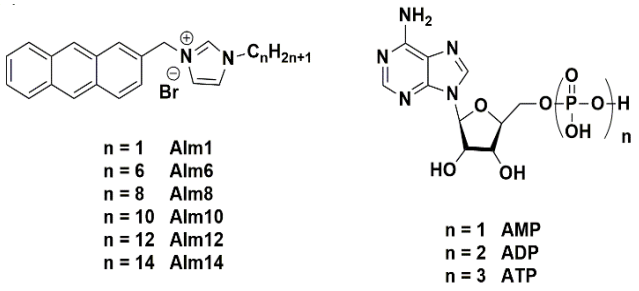

Figure 1. Structure of the compounds and nucleotides

This article is protected by copyright. All rights reserved.

Accepted Manuscript

10.1002/chem.202002648

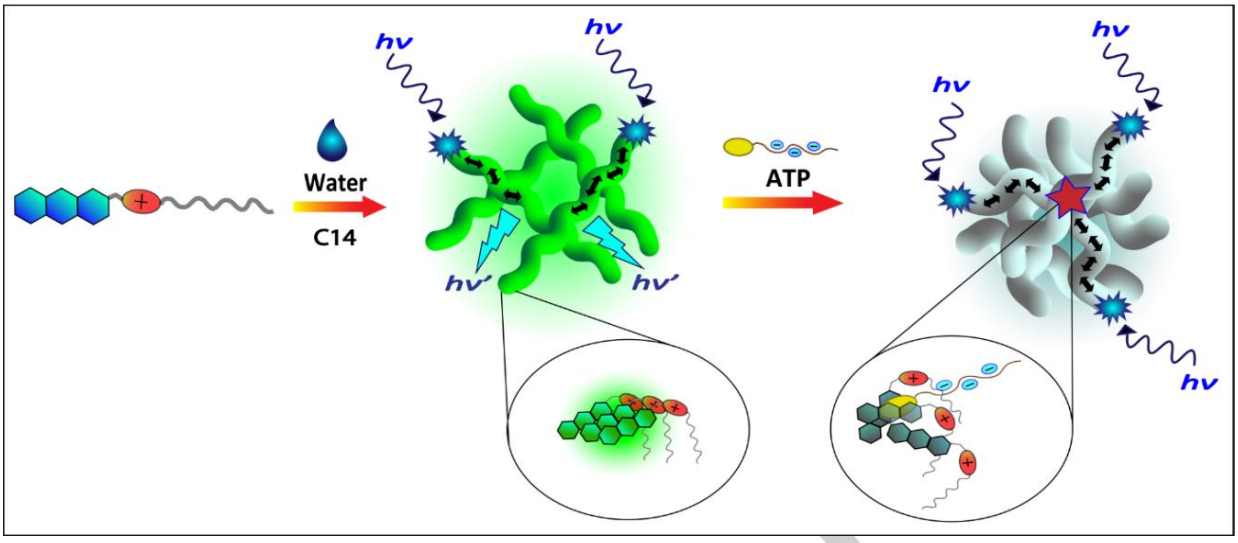

Scheme 1. A schematic representation of the self-assembly of **AIm14** and the amplified quenching by exciton migration upon ATP binding in its aggregates.

derivatives (N≥10), **AIm14**, in particular, showed an exceptionally amplified quenching leading to ATP detection at high picomolar concentrations. On the contrary, the non-assembled derivatives (**AIm1**, **AIm6**, **AIm8)**, did not sense ATP even at hundreds of micromolar concentrations. Thus, in comparison to these "molecular" receptors, the multivalent nanofibers of **AIm14** exhibited more than a million-fold higher sensitivity in ATP detection. Although such an amplified fluorescence quenching or superquenching has been known for CPEs,[21] what is truly remarkable is that in case of **AIm14**, the signal transduction occurred through non-covalently stacked chromophores in a supramolecular aggregate (Scheme 1). In addition, the multivalent nanofibers of **AIm14** also demonstrated an exceptional selectivity towards ATP over several other nucleotide tri-phosphates and pyrophosphate.

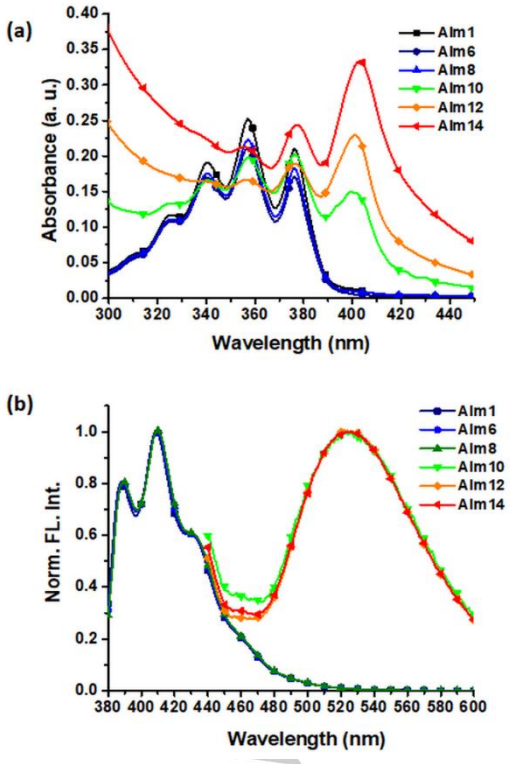

Figure 2. (a) Absorption and (b) emission spectra of **AIm1**, **AIm6** and **AIm8** (λ_{ex} 365 nm) and **AIm10**, **AIm12** and **AIm14** (λ_{ex} 400 nm) in buffer. The concentration of each derivative was 50 μM.

The **AImN** derivatives displayed attributes of monomeric anthracenes in their absorption and emission spectra in DMSO (Figure S3). However, in aqueous buffer (5 mM TRIS, 10 mM NaCl, pH 7.4), noticeable differences in the spectral features were observed depending on the chain-length (Figure 2). The derivatives with N≤8 chains (**AIm1**, **AIm6** and **AIm8**), exhibited similar spectral features as observed in DMSO (Figures 2 and S3), except small solvatochromic shifts. However, a new sharp, red-shifted absorption peak at 403 nm and an additional broad emission peak at 490 nm (Figures S6, S7 and S8) started to appear for **AIm10**, **AIm12** and **AIm14** in specific concentration ranges (1-10 μM for **AIm10** and **AIm12** and <1μM for **AIm14**). Scanning electron microscopy (SEM) images revealed the presence of entangled nano-fibrillar networks in these samples (Figures 3e and S23) which were absent for the smaller chain derivatives. These observations clearly suggested the self-assembly of N≥10 derivatives. The red-shifted absorption band suggested a J-like arrangement[22] of the stacked anthracenes whereas the large Stokes shift (87 nm) coupled with the broad feature of the emission band at 490 nm indicated that it was excimeric in origin. This was supported by its comparatively higher life-time than the monomeric emission (Table S2). The excitation spectra (λ_{em} = 490 nm) for these three derivative matched well with their absorption spectra (Figure S4) indicating

Table 1. Average size and zeta potential (ζ) of the self-assembled nanoaggregates of **AIm10**, **AIm12** and **AIm14** before and after addition of ATP in aqueous buffer from DLS measurements.

AImN	Size (nm) before ATP addition	Size (nm) after ATP (5 μM) addition	ζ (mV) before ATP addition	ζ (mV) after ATP (5 μM) addition
AIm10 (50 μM)	211 ± 21	354 ± 19	22.3 ± 2.8	9.5 ± 0.2
AIm12 (50 μM)	456 ± 35	639 ± 84	50 ± 3.1	16.5 ± 0.2
AIm14 (10 μM)	567 ± 23	868 ± 98	10.62±1.1	3.21±0.63

This article is protected by copyright. All rights reserved.

Accepted Manuscript

10.1002/chem.202002648

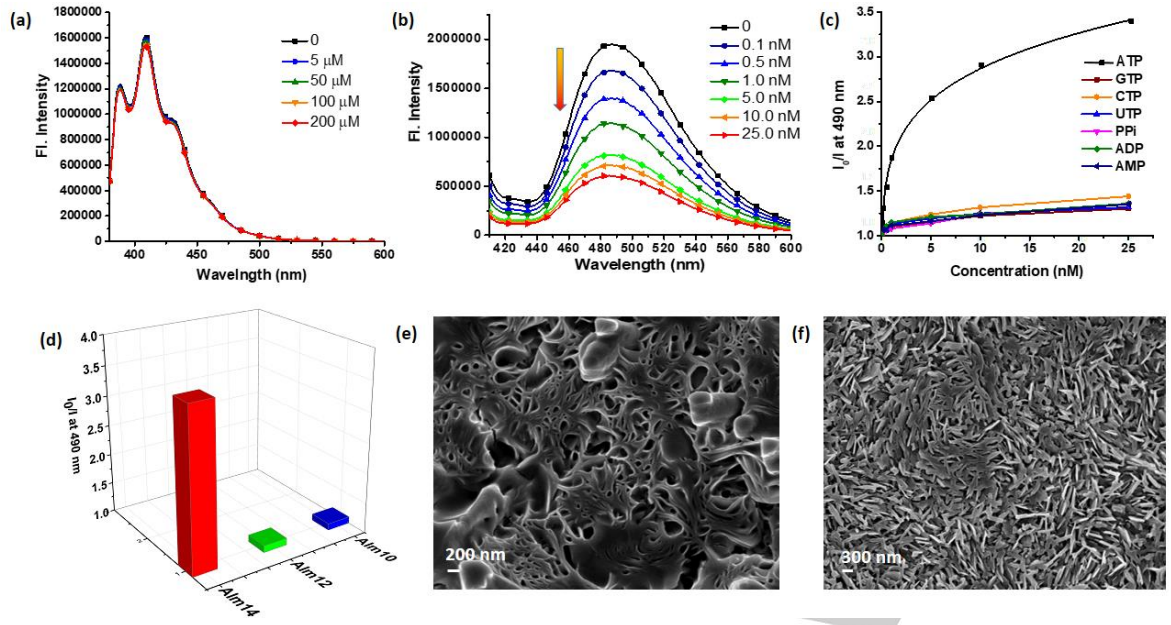

Figure 3. Fluorescence spectral changes of (a) **Alm1** (100 μM) and (b) **Alm14** (10 μM) upon addition of ATP and (c) **Alm14** (10 μM) upon addition ATP, PPi, ADP, AMP, UTP, CTP and GTP, (λ_{ex} 400 nm); (d) Comparative I_0/I values for **Alm10** (100 μM), **Alm12** (50 μM) and **Alm14** (10 μM) upon ATP (50 nM) addition; SEM images of **Alm14** (e) without ATP and (f) With ATP (5 μM).

that the excimers originated from the stacked anthracenes in the aggregates. The extent of aggregation, expectedly, was dependent on the ionic strength of the medium (Figure S5).

The nano-aggregates of all the three amphiphilic derivatives exhibited positive zeta potential values which decreased upon addition of ATP (Table 1). Also, the size of the nanoaggregates increased considerably upon ATP addition (Table 1) indicating the formation of larger co-aggregates. A visible morphological change was also observed in the SEM image (Figure 3f). These results, thus, clearly pointed out a multivalent mode of ATP binding. Most notably, ATP binding led to a quenching of both the monomer-like and excimeric emissions of the aggregates (Figure S13). This suggested that the monomer-like emission also resulted from the anthracenes in the stacks and not from the free monomers (*vide infra*). As the relative quenching of the excimer emission was comparatively higher, its emission changes were monitored. From a preliminary screening, the best response for each of the amphiphiles was obtained with the following concentrations: **Alm10**: 100 μM, **Alm12**: 50 μM and **Alm14**: 10 μM. Among them, the best sensitivity was exhibited by **Alm14** as ATP was detected at a concentration of 100 pM. The limit of detection (LOD) was 54 pM (Figure S20). The amplified quenching was illustrated by the fact that upon addition of 1 and 5 nM ATP (ATP/**Alm14** ratios of 1:10000 and 1:2000, respectively), around 40% and 60% excimer quenching[23] was observed (Figure 3b and S15. See Table S1 for the relative standard deviation (RSD) values). In case of **Alm10** and **Alm12**, the extent of quenching was noticeably lower (Figure 3d). For example, <10% quenching was observed with 5 nM of ATP for **Alm10** and **Alm12** (Figures S10, S11 and S14). We also studied the ATP-induced quenching in other buffer solutions such as PBS and it was observed that although in comparison to TRIS the response was slightly lower, nevertheless an efficient quenching was also observed in this case (Figure S18). In comparison to the multivalent aggregates, the smaller chain derivatives **Alm1**, **Alm6** and **Alm8** either showed negligible or no change in their monomeric emissions even after adding ATP till 200 μM (Figure 3a and S9). Therefore, in terms of the lower limit of detection, more than a million-fold increase in the sensitivity was demonstrated by the multivalent aggregates of **Alm14** compared to the "molecular" receptors. The lack of quenching in the monomeric receptors clearly indicated that multivalency and signal transduction played decisive roles in the ATP sensing by the aggregates. In case of conjugated polymers, amplified quenching or superquenching typically occurs through electron or energy transfer,[6] aggregation or conformational changes of the polymer upon analyte binding.[24] Amplified quenching was also reported for aggregated non-conjugated polymers with pendant dyes.[25] We believe that, the multivalent ATP binding induced a local co-aggregation of the supramolecular aggregates and this effect was more pronounced with the most hydrophobic **Alm14**.[26] The aggregation facilitated interchain migrations of the excitons which led to the amplification of the binding event. The quenching efficiency was found to be dependent on the concentration of **Alm14** in the aggregates and an optimum concentration (10 μM) gave the best results. At lower concentrations, the quenching was noticeably less (Figure S16). Also, above 10 μM, the extent of quenching remained almost same. These results thus indicated that the co-aggregate formation was the key to ATP induced quenching and an optimum concentration of the amphiphile was important. This was further supported by the studies at pH 3.5 in which the quenching was comparatively less than that observed at pH 7.4 (Figure S17). At a more acidic pH, the amount of negative charge on ATP was less and this would have hindered the formation of electrostatically driven co-aggregates to some extent. Notably, in terms of the lower limit of ATP detection, to our knowledge, the **Alm14** aggregates are superior not only to the reported multivalent self-assembled systems[19] but also those reported with CPEs.[27]

The multivalent aggregates of **Alm14** were subsequently employed to examine the binding selectivity of ATP compared to ADP and AMP, other nucleotide triphosphates (GTP, UTP and CTP) and pyrophosphate (PP_i) (Figure S2). In electrostatic charge density driven binding events, it is often difficult to achieve a high-level of selectivity between the nucleotide triphosphates. A plot of

This article is protected by copyright. All rights reserved.

Accepted Manuscript

10.1002/chem.202002648

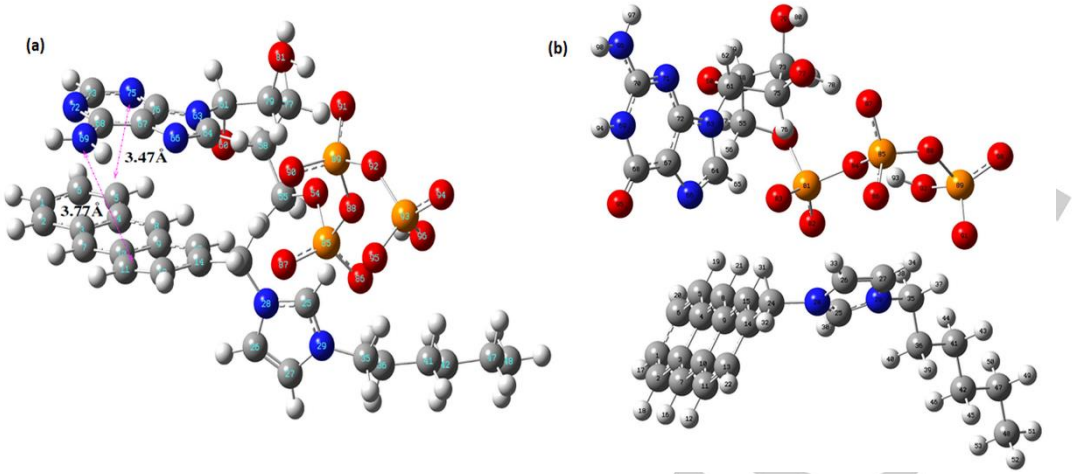

Figure 4. Optimized structure of (a) **AIm6** with ATP and (b) **AIm6** with GTP. Color coding: C: grey, H: white, N: blue, O: red, P: orange.

I_0/I (I_0 and I are the excimer intensities before and after the addition of phosphates) against concentration revealed that the **AIm14** nanoaggregates, in fact, showed an exceptional selectivity towards ATP in the nanomolar (Figure 3c. The error bars are shown in Figure S14) and as well as in the micromolar concentrations (Figure S12). Interestingly, the observed selectivity towards ATP by **AIm14** was not observed in other amphiphilic derivatives (see Figure S19 for **AIm12).** Although, the selectivity over ADP and AMP can be explained in terms of a comparatively weaker electrostatic binding, it was really intriguing to observe the binding selectivity of ATP over other nucleotide triphosphates having similar number of negative charges. In the literature, the selectivity of imidazolium based "molecular" receptors towards a particular nucleotide is typically attributed to the π-π stacking interactions between the nucleobase and the aromatic moieties.[20d,e, 28] In order to identify the existence of any such interaction in our case, we carried out computational analysis by comparing the interactions of **AIm6** with ATP and GTP. Although **AIm6** did not show multivalent ATP binding, it was chosen for computational feasibility. The ground state of **AIm6** with ATP and GTP (1:1 stoichiometry) was first optimized separately using Density Functional Theory (DFT) based on ωB97XD exchange correlation functional[29] and 6-311G (d,p) basis set[30] in Gaussian 09 program package.[31] A clear stacking between the anthracene ring of **AIm6** and the adenine ring of ATP was found whereas, in case of GTP, the guanine ring and the anthracene ring were quite apart from each other (Figure 4). Natural bond orbital (NBO) analysis using NBO 3.0[32] implemented in Gaussian 09 on these optimized structures revealed that there were two profound n→π* interactions between the adenine ring of ATP and the anthracene ring of **AIm6** (nN75 →π*C5-C6: 0.11 kcal/mol and nN69→π*C11-C13: 0.13 kcal/mol, Table S3). However, this interaction was absent in case of GTP. Subsequently, considering the multivalent mode of binding, we analyzed the interactions of **AIm6** dimer with ATP and GTP. NBO analysis on the optimized **AIm6** dimer showed three significant π-π* interactions between the anthracene rings (Figure S22a and Table S4). Thereafter, the **AIm6** dimer was optimized with ATP and GTP separately using ωB97xD/6-31G (d,p). NBO analysis on the composite structures of **AIm6** dimer/ATP and **AIm6** dimer/GTP showed that although there was a reduction in the π-π* interactions between the anthracene rings compared to **AIm6** dimer in both cases (Figures S22b and S22c and Table S4), an n-π* interaction existed between the adenine and one of the anthracene rings (Figure S22b, Table S2) in **AIm6** dimer/ATP. However, no such interaction was found for the guanine and anthracene in **AIm6** dimer/GTP. A couple of important points thus emerged from these studies: a) in the **AIm6** dimer, the slip-stacked arrangement of anthracenes correlated well with the observed J-band in the aggregates and b) the presence of an additional interaction between the adenine and anthracene might have contributed to the observed binding selectivity for ATP by the multivalent aggregates.

In conclusion, we have employed the self-assembly of amphiphilic imidazolium receptors to create multivalent supramolecular assemblies which showed a highly efficient signal transduction capability upon binding to ATP. The binding of ATP facilitated co-aggregate formation and quenched the excimeric emission of the stacked anthracenes. These quenching sites further acted as emission traps in the interconnected nanofibrillar networks and through exciton migration, one binding event led to the emission quenching of thousands of receptors. Apart from the amplified quenching features leading to a highly sensitive ATP detection, the other novel aspect of the multivalent aggregates was their remarkable selectivity towards ATP over other nucleotides. Our study shows that through the self-assembly of easily synthesizable small organic receptors, it is possible to create multivalent arrays which are equivalent to conjugated polymers in terms of the signal transduction and detection sensitivity and this approach thus offers an enormous potential for creating modular multivalent nanostructures for the recognition of many other biological targets. Furthermore, the presence of anthracene moiety in the amphiphiles provides an opportunity to tune the multivalent binding through photo-irradiation. Anthracenes are known to undergo photocycloaddition reactions in a reversible fashion and this can be utilized to control the multivalent binding of the aggregates towards ATP.

Acknowledgements

We are thankful to Science and Engineering Research Board (SERB), Department of Science and Technology (DST), Government of India (project: EMR/2016/002838) and Indian Institute of Science Education and Research Kolkata (Creation of Facility Grant) for support of this work. R.B. acknowledges IISER Kolkata for fellowship.

Conflict of Interest

This article is protected by copyright. All rights reserved.

Accepted Manuscript

The authors declare no conflict of interest.

Keywords: ATP • multivalency • signal transduction• self-assembly • sensors

[1] a) J. Huskens, L. J. Prins, R. Haag, B. J. Ravoo, *Multivalency: Concepts, Research and Applications*, John Wiley & Sons, New York, **2018**; b) C. Müller, G. Despras, T. K. Lindhorst, *Chem. Soc. Rev*. **2016**, *45*, 3275-3302; c) H. Choi, Y. Jung, *Chem. Eur. J*. **2018**, *24*, 19103–19109; d) J. L. J. Blanco, C. O. Mellet, J. M. G. Fernández, *Chem. Soc. Rev*. **2013**, *42*, 4518–4531.

[2] a) A. Mulder, J. Huskens, D. N. Reinhoudt, *Org. Biomol. Chem*. **2004**, *2*, 3409–3424; b) J. D. Badjic, A. Nelson, S. J. Cantrill, W. B. Turnbull, J. F. Stoddart, *Acc. Chem. Res*. **2005**, *38*, 723–732.

[3] M. Mammen, S. K. Choi, G. M. Whitesides, *Angew Chem. Int. Ed*. **1998**, *37*, 2754–2794.

[4] G. Krauss, *Biochemistry of Signal Transduction and Regulation*, Wiley–VCH, Weinheim, 3rd ed. **2008**, ch. 3, pp. 115–149.

[5] P. Scrimin, L. J. Prins, *Chem. Soc. Rev.* **2011**, *40*, 4488–4505.

[6] a) J. Liang, J. K. Lia, B. Liu, *Chem. Sci.* **2013**, *4*, 1377–1394; b) B. Liu, G. C. Bazan, *J. Am. Chem. Soc*. **2004**, *126*, 1942-1943; c) S. Rochat, T. M. Swager, *ACS Appl. Mater. Interfaces* **2013**, *5*, 4488−4502.

[7] a) S. W. Thomas III, G. D. Joly, T. M. Swager, *Chem. Rev.* **2007**, *107*, 1339-1386; b) X. Feng, L. Liu, S. Wang, D. Zhu, *Chem. Soc. Rev.* **2010**, *39*, 2411–2419.

[8] a) C. Fasting, C. A. Schalley, M. Weber, O. Seitz, S. Hecht, B. Koksch, J. Dernedde, C. Graf, E.-W. Knapp, R. Haag, *Angew. Chem. Int. Ed*. **2012**, *51*, 10472–10498; b) A. Barnard, D. K. Smith, *Angew. Chem. Int. Ed.* **2012**, *51*, 6572 – 6581.

[9] a) S. Malhotra, H. Bauer, A. Tschiche, A. M. Staedtler, A. Mohr, M. Calderón, V.S. Parmar, L. Hoeke, S. Sharbati, R. Einspanier, R. Haag, *Biomacromolecules* **2012**, *13*, 3087-3098; b) W. Drożdż, A. Walczak, Y. Bessin, V. Gervais, X.-Y. Cao, J.-M. Lehn, S. Ulrich, A. R. Stefankiewicz, *Chem. Eur .J.* **2018**, *24*, 10802–10811.

[10] a) S. M. Bromfield, D. K. Smith, *J. Am. Chem. Soc*. **2015**, *137*, 10056−10059; b) H. A. Behanna, K. Rajangam, S. I. Stupp, *J. Am. Chem. Soc*. **2007**, *129*, 321–327.

[11] a) B. S. Sandanaraj, D. R. Vutukuri, J. M. Simard, A. Klaikherd, R. Hong, V. M. Rotello, S. Thayumanavan, *J. Am. Chem. Soc.* **2005**, *127*, 10693-10698; b) V. Martos, P. CastreÇo, J. Valero, J. de Mendoza, *Curr. Opin. Chem. Biol.* **2008**, *12*, 698-706.

[12] X. Zhe, J. Shaorui, W. Wang, Z. Yuan, B. J. Ravoo, D.-S. Guo, *Nat. Chem*. **2019**, *11*, 86-93.

[13] a) S. Maiti, C. Pezzato, S. G. Martin, L. J. Prins, *J. Am. Chem. Soc*. **2014**, *136*, 11288−11291; b) S. Banerjee, B. König, *J. Am. Chem. Soc.* **2013**, *135*, 2967−2970.

[14] a) J. R. Knowles, *Annu. Rev. Biochem*. **1980**, *49*, 877–919; b) C. F. Higgins, I. D. Hiles, G. P. Salmond, D. R. Gill, J. A. Downie, I. J. Evans, I. B. Holland, L. Gray, S. D. Buckel, A.W. Bell, *Nature* **1986**, *323*, 448 – 450; c) A. V. Gourine, E. Llaudet, N. Dale, M. Spyer, *Nature* **2005**, *436*, 108-111.

[15] a) A. E. Hargrove, S. Nieto, T. Zhang, J. L. Sessler, E. V. Anslyn, *Chem. Rev.* **2011**, *111*, 6603–6782; b) N. Busschaert, C. Caltagirone, W. V. Rossom, P. A. Gale, *Chem. Rev*. **2015**, *115*, 8038−8155; c) A. M. Agafontsev, A. Ravi, T. A. Shumilova, A. S. Oshchepkov, E. A. Kataev, *Chem. Eur. J*. **2019**, *25*, 2684 – 2694.

[16] a) Y. Kurishita T. Kohira, A. Ojida, I. Hamachi, *J. Am. Chem. Soc.* **2012**, *134*, 18779−18789; b) H. N. Lee, Z. Xu, S. K. Kim, K. M. K. Swamy, Y. Kim, S.-J. Kim, J. Yoon, *J. Am. Chem. Soc*. **2007**, *129*, 3828-3829; c) E. A. Weitz, J. Y. Chang, A. H. Rosenfield, V. C. Pierre, *J. Am. Chem. Soc*. **2012**, *134*, 16099–16102; d) W. Fang, C. Liu, F. Yu, Y. Liu, Z. Li, L. Chen, X. Bao, T. Tu, *ACS Appl. Mater. Interfaces* **2016**, *8*, 20583-20590.

[17] a) D. Maity, M. Li, M. Ehlers, C. Schmuck, *Chem. Commun.* **2017**, *53*, 208–211; b) X. Li, X. Guo, L. Cao, Z. Xun, S. Wang, S. Li, Y. Li, G. Yang, *Angew. Chem. Int. Ed.* **2014**, *53*, 7809-7813; c) L. Wang, L. Yuan, X. Zeng, J. Peng, Y. Ni, J. C. Er, W. Xu, B. K. Agrawalla, D. Su, B. Kim, Y.-T. Chang, *Angew. Chem. Int. Ed.* **2016**, *55*, 1773 –1776.

[18] a) D. E. Huizenga, J. W. Szostak, *Biochemistry* **1995**, *34*, 656-665; b) X. Zuo, S. Song, J. Zhang, D. Pan, L. Wang, C. Fan, *J. Am. Chem. Soc*. **2007**, *129*, 1042-1043; c) E. D. Grosso, A. Idili, A. Porchetta, F. Ricci, *Nanoscale* **2016**, *8*, 18057–18061; d) S. Jhaveri, M. Rajendran, A. D. Ellington, *Nat. Biotechnol*. **2000**, *18*, 1293-1297.

[19] a) P. S. Muñana, G. Ragazzon, J. Dupont, C. Z. ‐ J. Ren, L. J. Prins, J. L.-Y. Chen, *Angew. Chem. Int. Ed*. **2018**, *57*, 16469 –16474; b) J. Liu, M. Morikawa, N. Kimizuka, *J. Am. Chem. Soc*. **2011**, *133*, 17370–17374; c) M. Onda, K. Yoshihara, H. Koyano, K. Ariga, T. Kunitake, *J. Am. Chem. Soc*. **1996**, *118*, 8524-8530; d) J.-H. Zhu, C. Yu, Y. Chen, J. Shin, Q.-Y. Cao, J. S. Kim, *Chem. Commun.* **2017**, *53*, 4342-4345; e) H. Jeon, S. Lee, Y. Li, S. Parka, J. Yoon, *J. Mater. Chem*. **2012**, *22*, 3795-3799; f) S. Banerjee, M. Bhuyan, B. König, *Chem. Commun*. **2013**, *49*, 5681-5683; g) J. F. Neal, W. Zhao, A. J. Grooms, M. A. Smeltzer, B. M. Shook, A. H. Flood, H. C. Allen, *J. Am. Chem. Soc*. **2019**, *141*, 19, 7876-7886.

[20] a) N. Ahmed, B. Shirinfar, I. S. Youn, A. Bist, V. Suresh, K. S. Kim, *Chem. Commun.* **2012**, *48*, 2662 –2664; b) N. Ahmed, B. Shirinfar, I. Geronimo, K. S. Kim, *Org. Lett*. **2011**, *13*, 5476– 5479; c) D. H. Wang, X. L. Zhang, C. He, C. Y. Duan, *Org. Biomol. Chem*. **2010**, *8*, 2923 –2925; d) J. Y. Kwon, N. J. Singh, H. N. Kim, S. K. Kim, K. S. Kim, J. Yoon, *J. Am. Chem. Soc*. **2004**, *126*, 8892-8893; e) Z. Xu, N. J. Singh, J. Lim, J. Pan, H. N. Kim, S. Park, K. S. Kim, J. Yoon, *J. Am. Chem. Soc*. **2009**, *131*, 15528–15533.

[21] a) L. Chen, D. W. McBranch, H.-L. Wang, R. Helgeson, F. Wudl, D. G. Whitten, *PNAS*, **1999**, 96, 12287–12292; (b) Q. Zhou, T.M. Swager, *J. Am. Chem. Soc*. **1995**, *117*, 12593-12602; (c) C. Fan, S. Wang, J. W. Hong, G. C. Bazan, K. W. Plaxco, A. J. Heeger, *PNAS*, **2003**, *100*, 6297–6301; (d) K. E. Achyuthan, T. S. Bergstedt, L. Chen, R. M. Jones, S. Kumaraswamy, S. A. Kushon, K. D. Ley, L. Lu, D. McBranch, H. Mukundan, F. Rininsland, X. Shi, W. Xia, D. G. Whitten, *J. Mater. Chem.* **2005**, *15*, 2648–2656.

[22] F. Würthner, T. E. Kaiser, C. R. Saha-Möller, *Angew. Chem. Int. Ed*. **2011**, *50*, 3376-3410.

[23] The quenching of the monomer-like band at 412 nm was ~50% at 5 nM ATP.

[24] a) A. Satrijo, T. M. Swager, *J. Am. Chem. Soc*. **2007**, *129*, 16020-16028; b) C. Tan, E. Atas, J. G. Müller, M. R. Pinto, V. D. Kleiman, K. S. Schanze, *J. Am. Chem. Soc*. **2004**, *126*, 13685-13694;

[25] R. M. Jones, L. Lu, R. Helgeson, T. S. Bergstedt, D. W. McBranch, D. G. Whitten, *PNAS*, **2001**, *98*, 14769–14772.

[26] F. Xia, X. Zuo, R. Yang, Y. Xiao, D. Kang, A. Vallée-Bélisle, X. Gong, A. J. Heeger, K. W. Plaxco, *J. Am. Chem. Soc*. **2010**, *132*, 1252–1254.

[27] a) C. Li, M. Numata, M. Takeuchi, S. Shinkai, *Angew. Chem. Int. Ed*. **2005**, *44*, 6371 –6374; (b) Q. Cui, Y. Yang, C. Yao, R. Liu, L. Li, *ACS Appl. Mater. Interfaces* **2016**, *8*, 35578−35586; (c) D. Cheng, Y. Li, J. Wang, Y. Sun, L. Jin, C. Lib, Y. Lu, *Chem. Commun*. **2015**, *51*, 8544—8546; (d) Q. Zhao, Z. Zhang, Y. Tang, *Chem. Commun*. **2017**, *53*, 9414—9417.

[28] E. A. Kataev, T. A. Shumilova, B. Fiedler, T. Anacker, J. Friedrich, *J. Org. Chem*. **2016**, *81*, 6505−6514.

[29] J. D. Chai, M. H. Gordon, *Phys. Chem. Chem. Phys*. **2008**, *10*, 6615-6620.

[30] R. Ditchfield, W. J. Hehre, J. A. Pople, *J. Chem. Phys*. **1971**, *54*, 724-728.

[31] M. J. Frisch, G. W. Trucks, H. B. Schlegel, G. E. Scuseria, M. A. Robb, J. R. Cheeseman, G. Scalmani, V. Barone, B. Mennucci, G. A. Petersson, H. Nakatsuji, M. Caricato, X. Li, H. P. Hratchian, A. F. Izmaylov, J. Bloino, G. Zheng, J. L. Sonnenberg, M. Hada, M. Ehara, K. Toyota, R. Fukuda, J. Hasegawa, M. Ishida, T. Nakajima, Y. Honda, O. Kitao, H. Nakai, T. Vreven, Jr. J. A. Montgomery, J. E. Peralta, F. Ogliaro, M. Bearpark, J. J. Heyd, E. Brothers, K. N. Kudin, V. N. Staroverov, R. Kobayashi, J. Normand, K. Raghavachari, A. Rendell, J. C. Burant, S. S. Iyengar, J. Tomasi, M. Cossi, N. Rega, J. M. Millam, M. Klene, J. E. Knox, J. B. Cross, V. Bakken, C. Adamo, J. Jaramillo, R. Gomperts, R. E. Stratmann, O. Yazyev, A. J. Austin, R. Cammi, C. J. Pomelli, W. Ochterski, R. L. Martin, K. Morokuma, V. G. Zakrzewski, G. A. Voth, P. Salvador, J. J. Dannenberg, S. Dapprich, A. D. Daniels, O. Farkas, J. B. Foresman, J. V. Ortiz, J. Cioslowski, Gaussian 09, revision D.01; Gaussian, Inc.: Wallingford, CT, **2009**.

[32] E. D. Gendening, A. E. Reed, J. E. Carpenter, F. Weinhold, NBO 3.0 Program Manual. Theoretical Chemistry Institute, University of Wisconsin, Madison, WI, **1990**.

Accepted Manuscript

This article is protected by copyright. All rights reserved.

10.1002/chem.202002648

Entry for the Table of Contents

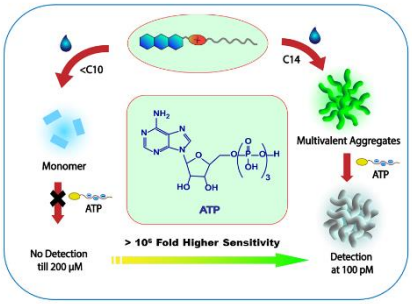

Anthracene tagged amphiphilic imidazolium receptors undergo self-assembly in aqueous media to form multivalent nano-aggregates which bind ATP. The multivalent binding leads to an amplified quenching of the excimeric emission of the stacked anthracenes through an efficient signal transduction. A highly sensitive detection of ATP was achieved along with an exceptional selectivity over several other nucleotide triphosphates.

WILEY-VCH

Accepted Manuscript

This article is protected by copyright. All rights reserved.